Journal for ImmunoTherapy of Cancer

Identification of neuroblastoma cell lines with uncommon TAZ+/mesenchymal stromal cell phenotype with strong suppressive activity on natural killer cells

Claudia Canzonetta,[1] Andrea Pelosi [iD] ,[1] Sabina Di Matteo [iD] ,[1] Irene Veneziani,[1] Nicola Tumino,[1] Paola Vacca,[1] Enrico Munari,[2,3] Marco Pezzullo,[4] Charles Theuer,[5] Rita De Vito,[6] Vito Pistoia,[1] Luigi Tomao,[7] Franco Locatelli,[7,8] Lorenzo Moretta,[1] Ignazio Caruana [iD] ,[7,9] Bruno Azzarone [iD] [1]

ABSTRACT

Background Neuroblastoma (NB) is the most common, extracranial childhood solid tumor arising from neural crest progenitor cells and is a primary cause of death in pediatric patients. In solid tumors, stromal elements recruited or generated by the cancer cells favor the development of an immune-suppressive microenvironment. Herein, we investigated in NB cell lines and in NB biopsies, the presence of cancer cells with mesenchymal phenotype and determined the immune-suppressive properties of these tumor cells on natural killer (NK) cells.

Methods We assessed the mesenchymal stromal cell (MSC)-like phenotype and function of five human NB cell lines and the presence of this particular subset of neuroblasts in NB biopsies using flow-cytometry, immunohistochemistry, RT-qPCR, cytotoxicity assays, western blot and silencing strategy. We corroborated our data consulting a public gene-expression dataset.

Results Two NB cell lines, SK-N-AS and SK-N-BE(2)C, exhibited an unprecedented MSC phenotype (CD105+/CD90+/CD73+/CD29+/CD146+/GD2+/TAZ+). In these NB-MSCs, the ectoenzyme CD73 and the oncogenic/immune-regulatory transcriptional coactivator TAZ were peculiar markers. Their MSC-like nature was confirmed by their adipogenic and osteogenic differentiation potential. Immunohistochemical analysis confirmed the presence of neuroblasts with MSC phenotype (CD105+/CD73+/TAZ+). Moreover, a public gene-expression dataset revealed that, in stage IV NB, a higher expression of TAZ and CD105 strongly correlated with a poorer outcome. Among the NB-cell lines analyzed, only NB-MSCs exhibited multifactorial resistance to NK-mediated lysis, inhibition of activating NK receptors, signal adaptors and of NK-cell cytotoxicity through cell-cell contact mediated mechanisms. The latter property was controlled partially by TAZ, since its silencing in NB cells efficiently rescued NK-cell cytotoxic activity, while its overexpression induced opposite effects in non-NB-MSC cells.

Conclusions We identified a novel NB immunoregulatory subset that: (i) displayed phenotypic and functional properties of MSC, (ii) mediated multifactorial resistance to NK-cell-induced killing and (iii) efficiently inhibited, in coculture, the cytotoxic activity of NK cells against target cells through a TAZ-dependent mechanism. These findings indicate that targeting novel cellular and molecular components may disrupt the immunomodulatory milieu of the NB microenvironment ameliorating the response to conventional treatments as well as to advanced immunotherapeutic approaches, including adoptive transfer of NK cells and chimeric antigen receptor T or NK cells.

BACKGROUND

Neuroblastoma (NB) is a pediatric tumor of the peripheral adrenergic lineage, which originates from neural crest. It is the most common malignancy diagnosed in infants[1] and the most frequent extracranial solid tumor in children, accounting for about 15% of pediatric tumor deaths.[2] Factors influencing patient's outcome include age at presentation, histology, MYCN status and tumor stage at diagnosis.[3] Patients with NB present with metastatic disease in approximately a half of cases.[4]

Treatment of patients with relapsed stage IV NB remains a major challenge, with less than 10% of children surviving disease free at 5 years after recurrence.[5] However, novel therapies targeting biologically relevant pathways and recent immunotherapeutic approaches may provide new opportunities for improving the currently dismal patient outcome.[6 7]

Natural killer (NK) cells are a key component of the innate immune system. They lyse cancer cells, control metastases and represent a promising weapon against aggressive tumors such as NB.[8] However, human

BMJ

NB cells display multiple immune evasion mechanisms capable of impairing antitumor responses of both innate and adaptive immune cells, such as generation of an inhibitory tumor microenvironment (TME) and further recruitment of immunosuppressive cells.[8 9] In this regard, cancer-associated fibroblasts (CAF) and tumor-associated mesenchymal stromal cells (MSC) frequently generate an immunosuppressive microenvironment that impairs anti-tumor immunity.[10 11]

In NB, it has recently been shown that TME is infiltrated by stromal cells termed CAF-MSC that display powerful protumorigenic properties and inhibitory potential on T lymphocytes.[12 13] Interestingly, in this context, the human nephroblastoma stromal component derived from tumor tissue display genetic alterations identical to those present in tumor cells.[14] However, NB cells with immune-regulatory properties have not been investigated yet. Recently, NB has been described to be composed of two different tumor cell types with divergent gene expression profiles: committed adrenergic cells and CD133^{+} undifferentiated, "primitive" MSC, which are enriched in relapses and are more resistant to chemotherapeutic agents *in vitro*.[15]

Interestingly, primitive mesenchymal NB cells differentially express the transcriptional coactivator WW domain-containing transcription regulator-1 (WWTR1 also known as TAZ), which controls differentiation of MSC.[15 16] TAZ and its paralog YAP are important effectors of Hippo signaling pathway, which has pro-tumorigenic and immune-regulatory effects in multiple tumors.[17–20] They have been reported to be also implicated in NB invasiveness and dissemination.[16 21] Moreover, Cordenonsi *et al* recently demonstrated that the activity of TAZ is required to sustain self-renewal and tumor-initiation capacities of breast cancer stem cells.[22]

Here, we show that out of five NB cell lines, two of them, SK-N-AS and SK-N-BE(2)C, display: (1) phenotypic and functional properties typical of MSC; (2) multifactorial resistance to NK-cell-mediated killing and (3) inhibitory activity on NK-cell cytotoxicity, an effect requiring cell-cell contact in coculture. In these tumors, TAZ silencing could re-establish, on coculture with NB-MSCs, the cytotoxic activity of NK cells against the NK-sensitive K-562 target cells, whereas its transient overexpression induced opposite effects in non-NB-MSC cells.

These data provide the first identification of a new NB-cell subset displaying immunosuppressive properties and a novel promising target for innovative NB treatment.

MATERIAL AND METHODS
Cell lines
SK-N-AS, SK-N-BE(2)C, SH-SY5Y, IMR-32 and HTLA-230 human NB-cell lines and human erythroleukemia cell line K-562 were purchased from the American Type Culture Collection (ATCC, Manassas, Virginia, USA). HTLA-230, IMR-32 and SK-N-AS were grown in Dulbecco's Modified Eagle Medium high glucose (Euroclone, Milan, Italy).

SK-N-BE(2)C, SH-SY5Y and K-562 were grown in Roswell Park Memorial Institute (RPMI) -1640 medium (Euroclone). Cell culture media were supplemented with 2 mM L-glutamine (Euroclone), 1% penicillin and streptomycin (Euroclone) and 10% fetal bovine serum (FBS; Thermo-Fisher Scientific, Waltham, USA). Primary bone marrow-derived mesenchymal stromal cells (BM-MSC) were isolated and cultured as previously described.[23] Cell lines were certified for their identity by PCR-single-locus-technology (Eurofins-Genomics, Ebersberg, Germany). Cultures were periodically tested to confirm the absence of Mycoplasma by Mycoplasma Detection Kit (Venor-GeM Advance, Berlin, Germany). The different NB cell lines were employed within a limited number of passages after their acquisition from ATCC: SHSY5Y (4–20), IMR32 (8–18), SKNAS (7–28), SKNBE2c (3–14) HTLA (4–12). During their period of utilization, the different NB cell lines maintained a stable phenotype. Their genetic status concerning MYCN, 1p36 and p53 amplification/mutation is summarized in online supplemental table 1.

Purification of NK cells
Fresh NK cells were isolated from peripheral blood mononuclear cells (PBMC) obtained from buffy coats as previously described.[24] To obtain polyclonal activated NK (aNK) cells, freshly isolated NK cells were cultured on 30 Gy irradiated allogeneic PBMC feeder cells in the presence of 600 U/mL recombinant human IL-2 (Proleukin; Novartis-Farma, Origgio, Italy) and 1.5 ng/mL phytohemagglutinin (Merck-Millipore, Burlington, USA) for the first week, as previously described.[24] aNKs were used to perform experiments during the exponential growth phase.

Human samples
Buffy coats were collected from volunteer blood donors admitted to the blood transfusion service of OPBG after obtaining informed consent. The Ethical Committee of OPBG approved the study (825/2014) that was conducted in accordance with the ethical principles stated in the Declaration of Helsinki.

Flow-cytometry
For detection of surface markers, NB or NK cells were stained with the fluorochrome-conjugated monoclonal antibodies (mAbs) listed in online supplemental table 2 for 20 min at 4°C. For detection of intracellular markers, NK cells were treated with the BD-Cytofix/cytoperm kit (BD-Biosciences, San Jose, USA) according to manufacturer's protocols and stained with indicated mAbs.

Cells were acquired with the Beckman-Coulter Cytoflex-S flow-cytometer (Beckman-Coulter, Brea, USA). A minimum of 5000 events for each condition were acquired. The acquired data were analyzed with CytExpert-2.3 (Beckman-Coulter) and FlowJo V.10 software (BD-Biosciences).

Data were shown as mean fluorescence intensity ratio (MFI Ratio-mAb/unstained). Otherwise, the data were

shown as Fold Change MFI, which represents the ratio between the sample stained with the selected mAb and the control stained with the selected mAb.

Western blot (WB)

Total protein extracts were fractionated by SDS-PAGE gel electrophoresis (4%–12% Bis-Tris Polyacrylamide) and transferred to a nitrocellulose blotting membrane 0.45 µm. For TAZ detection, the protein extract was incubated with mAbs indicated in online supplemental table 2 and diluted as indicated following the manufacturer's instructions. Signals were developed with SuperSignal West Dura Extended Duration Substrate (Thermo-Fisher Scientific) according to manufacturer's instruction and detected with the Uvitec-Mini-HD9 technology (Uvitec, Dubai, UAE). Densitometry was performed using the ImageJ-1.51 software (National Institutes of Health).

Differentiation assays

For adipogenic and osteogenic differentiation, NB cell lines were plated and cultured in 6-well plates until 80% of confluence. Differentiation medium for adipogenesis was RPMI-1640 Medium supplemented with 10% FBS, 0.5 µM dexamethasone, 50 mg/mL L-ascorbic acid, 5 mM β-glycerol phosphate, 0.5 mM 3-Isobutyl-1-methylxanthine (Sigma-Aldrich, St. Louis, USA), 50 µM indomethacin (MP-Biomedicals, Huissen, Netherlands). Medium was changed two times a week and differentiation was evaluated after 21 days. The adipogenic cultures were fixed in 10% formalin (Sigma-Aldrich) for 1 hour and stained with fresh Oil Red O solution for 2 hours. The Oil Red O solution was prepared by mixing three parts stock solution (0.5% in isopropanol; Sigma-Aldrich) with two parts water. Plates were washed with Dulbecco's Phosphate Buffered Saline (DPBS) and dried before analysis. Adipogenic differentiation was confirmed by the appearance of fat droplets. Osteogenic differentiation medium consisted of RPMI supplemented with 10% FBS, 50 ng/mL L-thyroxine, 20 mM β-glycerol phosphate, 100 nM dexamethasone and 50 µM L-ascorbic acid (Sigma-Aldrich). The osteogenic cultures were fixed in 10% formalin for 1 hour and calcium deposits were revealed by 10% Alizarin Red S staining (Sigma-Aldrich).

Immunohistochemistry (IHC) studies

A 2.5 µm of overflow paraffin-embedded NB tissues from OPBG's patients and NB tissue microarray with duplicate cores per case (NB642A, Biomax Planegg, Germany) were deparaffinized and the antigenic epitopes were unmasked by PT link (DAKO, Bazzano, Italy). Endogenous peroxidase activity was blocked by incubating in 3% H_2O_2 solution in methanol. Non-specific sites were blocked with 5% Bovine Serum Albumin (BSA) and 1% goat serum in DPBS. Slides were incubated with mAbs indicated in online supplemental table 2 in a humidified chamber at room temperature overnight. For detection, Dako EnVision FLEX Mini Kit (Dako) was used followed by counterstaining with Gill's Hematoxylin. IHC slides

were subsequently scanned by NanoZoomer S60-Digital slide scanner (Hamamatsu-Photonics, Hamamatsu, Japan). The images were processed by NDP.view2 software (Hamamatsu-Photonics) for the identification of the same tumor area.

OPBG's patient data are summarized in online supplemental table 3.

Cytotoxicity assays

NK cells were tested for cytolytic activity in a flow-cytometric assay for NK-cell killing. NB or K-562 cells were used as targets for NK cell functional assays and different Effector:Target (E:T) ratios were tested. Briefly, NB or K-562 cells were stained with 5 µM Cell Tracker Green (CMFDA; Thermo-Fisher Scientific) and plated at 5000 cells/V-bottom 96-microwell plates. Target cells were incubated with NK cells at 37°C at different E:T ratios. After 4 hours of incubation, propidium iodide (PI, Sigma-Aldrich) was added. Cells were acquired with the Beckman-Coulter Cytoflex-S flow cytometer and live target cells were identified as CMFDA$^+$ PI$^-$, whereas dead target cells were CMFDA$^+$ PI$^+$. Percentage (%) of cell lysis was calculated as follows:

$$\% \text{ cell lysis} = \frac{(\% \text{ of dead cells cultured with NK}) - (\% \text{ of spontaneous lysis})}{100 - (\% \text{ of spontaneous lysis})} \times 100$$

Coculture of NK and target cells

For coculture experiments freshly isolated NK cells were cultured (3×10^5 cells/well) with 600 U/mL of IL-2 either alone or in the presence of NB cell lines (10^5 cells/well) in 24-wells plates in a 3:1 ratio. For transwell culture conditions, we used insert for 24-well plate with Polyester (PET) membrane bottom and pore size 0.4 µm (Sarstedt, Nümbrecht, Germany). Freshly isolated NK cells were seeded in the upper insert (3×10^5 cells/well) and both NB (10^5 cells/well) and NK cells were seeded in the lower chamber (3×10^5 cells/well) using a 3:1 ratio.

In the experiments with indoleamine 2,3-dioxygenase (IDO) and Prostaglandin E$_2$ (PGE2) synthesis inhibitors, in addition to 600 U/mL of IL-2 for 4 days, as previously described,[25] we used: 1 mM of 1-methyl-tryptophan (Sigma-Aldrich, an IDO inhibitor capable to block kynurenine production) and 5 µM NS-398 (Sigma-Aldrich, an inhibitor of PGE2 synthesis). NK cells were collected and used as effectors in the cytotoxicity assays. K-562 cell line was used as control target for NK cell functional assays.

Masking experiments

NK cells were tested for cytolytic activity against target cell lines in a 4 hours ^{51}Cr-release assay. Briefly, target cells were marked with 15 µCi and plated at 5×10^3 cells/well in 96-well V-bottom microplates. Then, NK cells were added at indicated E:T ratios in the presence of 5 µg/mL of purified anti-B7-H3 (M5B14) IgM blocking antibody in media.[26] Fifty microliters of hybridoma supernatant anti–HLA class I (A6.136) IgM was used for masking HLA class I.[27] IgM mAb (R&D Systems, Minneapolis, USA) was used as control.

For antibody-dependent cellular cytotoxicity (ADCC) assay, we employed the anti-CD105 IgG TRC105 (Carotuximab, Tracon-Pharmaceuticals, San Diego, USA) and the anti-GD2 IgG dinutuximab beta (Eusa Pharma, Amsterdam, Netherlands). NK cells were tested for cytolytic activity against the NB cell lines in a 4 hours ^{51}Cr-release assay in the presence of 10 µg/mL of purified anti-CD105 mAb, 100 µg/mL of purified anti-GD2 mAb as previously reported[28] or IgG mAb (R&D Systems). For ADCC with anti-CD105, BM-MSC was used as positive control.

At the end of 4 hours, the supernatant was collected and the radioactivity measured by a gamma counter (Microbeta2, PerkinElmer).

Data were expressed as: $\% \text{ of cell lysis} = \left[\frac{x-min}{max-min}\right] \times 100$.

Min represent minimum of recorded hits measured as target basal dead without NK. Max represents maximum of recorded hits, and it was measured as target maximum ^{51}Cr released after total lysis with Triton X-100.

Small interfering RNAs and cell transfections

NB cell lines SK-N-AS and SH-SY5Y were transfected with Lipofectamine-3000 reagent (Thermo-Fisher Scientific). 60%–70% confluent cells were detached with Trypsin-EDTA, resuspended in complete growth medium with 30 pmol/well of siRNA or 0.5 µg/well of plasmid DNA in Lipofectamine mix solution prepared following manufacturer's instructions. 2×10^5 cells were reseeded in 24-wells and transfection efficiency was evaluated at different times, as indicated. Gene silencing of TAZ and CD73 was performed with Silencer-Select predesigned siRNAs. The following siRNA oligonucleotides were used: siRNA1-TAZ (siWWTR1-s24788), siRNA2-TAZ (siWWTR1-s24789), siRNA1-CD73 (siNT5E-s9735), siRNA2-CD73 (siNT5E-s9736) and siRNA-Ctrl used as negative control (Life Technologies). TAZ overexpression was performed with pLL3.7-EGFPC2 TAZ mammalian expression vector. Cells transfected without DNA or with plasmid vector encoding GFP only were used as mock control, as indicated. pLL3.7-EGFPC2 TAZ was a gift from Yutaka Hata (Addgene plasmid # 66850).[29]

Quantitative real time quantitative-PCR (RT-qPCR) analysis

Total RNA extraction from NB cells was performed with miRNeasy mini kit with on-column DNase-I treatment following manufacturer's protocol (Qiagen, Hilden, Germany). 500 ng of total RNA was reversely transcribed with random primers by using Super Script IV first-strand synthesis system following manufacturer's instructions (Thermo-Fisher Scientific). RT-qPCRs were carried out in triplicates with PowerUp Sybr-Green reagent (Applied-Biosystems, Foster City, USA). Glyceraldehyde 3-phosphate dehydrogenase (GAPDH) was used as endogenous controls. RT-qPCRs were run on a QuantStudio-6 Flex instrument (Applied-Biosystems). Expression values were obtained by ΔΔCt method using QuantStudio Real-TimePCR-system software v.1.3.

Online supplemental table 4 indicates primers used in the study.

Statistical analysis

Data were expressed as mean±SD or ±SE, as indicated. Statistical significance was calculated using the Student's two-tailed T-test with Bonferroni correction for multiple comparisons, as indicated. P<0.05 were considered statistically significant. Data were graphed using GraphPad Prism 6 software (GraphPad Software). The overall survival (OS) and event-free survival (EFS) probabilities were calculated using the Kaplan-Meier survival curves with a log-rank test with Bonferroni correction to
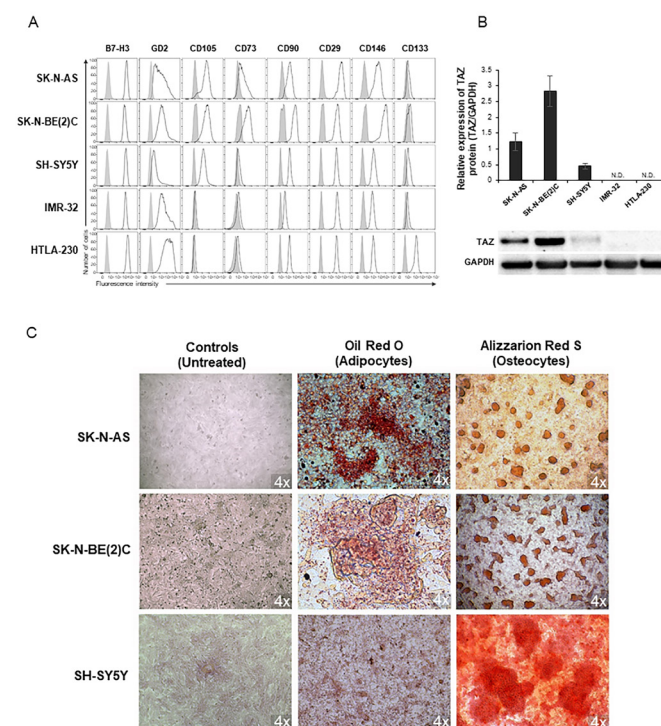

Figure 1 Evaluation of the mesenchymal phenotype in NB cell lines. (A) Flow-cytometry analysis of the indicated MSCs and NB surface markers in NB cell lines. Gray histograms represent unstained controls, and white histograms represent stained samples. A representative experiment is shown of n=5 experiments performed. (B) WB of TAZ expression in different NB cell lines. GAPDH was used as loading control. Histograms represent the relative quantification of TAZ protein expression normalized for GAPDH. Data are expressed as mean±SD (n=3) (upper panel). A representative WB experiment is shown (lower panel). (C) Optical microscope photographs showing osteogenic and adipogenic differentiation capacity of putative NB-MSCs cell lines. Controls are represented by the NB lines cultured in their own medium. The differentiation into adipocytes is revealed by the formation of lipid droplets stained with Oil Red O. The differentiation into osteoblasts is documented by the detection of calcium depositions positive for Alizarin Red S. Original magnification 4×. The photos are representative of n=3 independent experiments. MSC, mesenchymal stromal cell; NB, neuroblastoma; WB, Western blot.
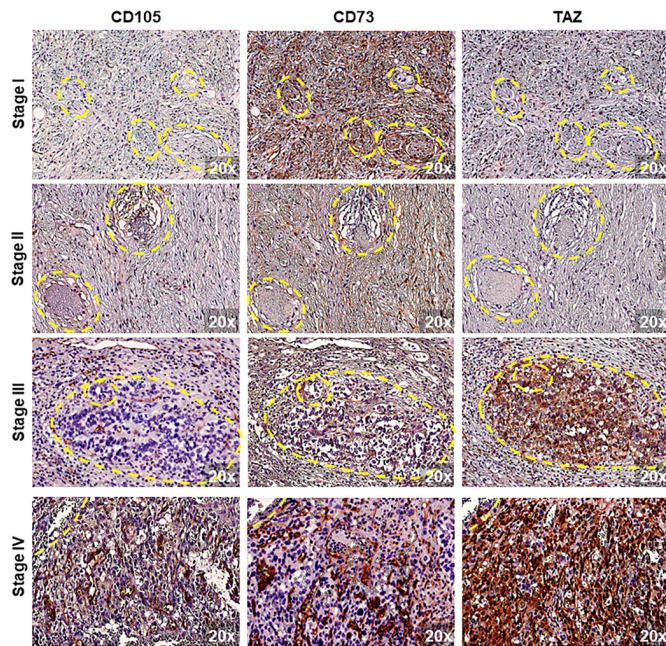
Figure 2 Expression of CD105, CD73 and TAZ in human NB tissue sections by IHC. Representative images of sections of 6 NB tumors from OPBG's donors and 27 cases of NB tissue microarrays (n=33) stained for CD105, CD73 and TAZ. 20× magnification was used for each image. Dashed yellow lines indicate the same areas in the different tumor sections analyzed. Vascular structures and rare stromal elements stained positive for CD105 and CD73 markers in all samples. IHC, immunohistochemistry; NB, neuroblastoma.

measure differences between stages using tools present in R2 dataset (http://r2.amc.nl). The samples were divided in high versus low antigen expression using the last quartile of their distribution as cut-off.

RESULTS
SK-N-AS and SK-N-BE(2)C cell lines exhibit a MSC phenotype
To evaluate the MSC phenotype of different NB cells, we analyzed five commercially available human cell lines (SK-N-AS, SK-N-BE(2)C, SH-SY5Y, IMR-32 and HTLA-230) by flow-cytometry for the expression of the NB surface markers B7-H3 and GD2, the MSC markers CD105, CD73, CD90, CD29, CD146 and the stem cell marker CD133 (figure 1A) and for the intracellular MSC marker TAZ by WB (figure 1B).

We observed that all cells of the five cell lines analyzed expressed B7-H3 and GD2, thus confirming that they are homogeneously composed of NB tumor cells (figure 1A). In addition, we found that all expressed CD90, CD29 and CD146, although at different levels. Based on the expression of CD105, CD73 and TAZ, we could identify three types: SK-N-AS and SK-N-BE(2)C with a well-defined MSC phenotype (NB-MSC, CD105$^+$/CD73$^+$/TAZ$^+$), SH-SY5Y which lacked the expression of some MSC markers (CD105$^+$/CD73$^-$/TAZ^{dull}), and IMR-32 and

HTLA-230 with no MSC markers (CD105$^-$/CD73$^-$/TAZ$^-$) (figure 1A,B). Of note, only HTLA-230 cell line expressed the stem cell marker CD133 (figure 1A).

The phenotypic similarity of SK-N-AS and SK-N-BE (2)C with MSCs raised the question of whether MSC-like NB cells could display the differentiation potential typical of MSCs. To address this question, we performed in vitro differentiation experiments. After 5 weeks of culture in adipogenic medium, induction of adipocyte differentiation was assessed using Oil Red O staining. In comparison with untreated control cultures (figure 1C, left panels), SK-N-AS and SK-N-BE(2)C, but not SH-SY5Y, showed strong Oil Red O staining (figure 1C, middle panels). Osteogenic differentiation was analyzed by Alizarin Red S uptake, according to an osteogenic stimulation protocol. All three cell lines formed mineralized nodules (figure 1C, right panels). In contrast, neither IMR-32 nor HTLA-230 exhibited differentiation potential (data not shown).

Based on these data, we conclude that both SK-N-AS and SK-N-BE(2)C may be classified as NB-MSC.

NB-MSC are present in primary NB samples and inversely correlate with the clinical outcome
In order to analyze whether MSCs are present in primary NB tissues, we performed IHC using primary overflow sections from four patients using commercially available NB tissue microarrays. Analysis of the expression of CD105, CD73 and TAZ revealed a different marker intensity and distribution depending on the tumor stage. CD73 was expressed in all stages with the higher intensity in samples of patients with stage IV disease. In stage IV patient samples, also coexpression of CD105 and TAZ was detected (figure 2). CD105 was predominantly expressed samples of patients with stage IV NB, while the levels of TAZ increased (both in terms of positive cells and intensity) from stage I to IV.
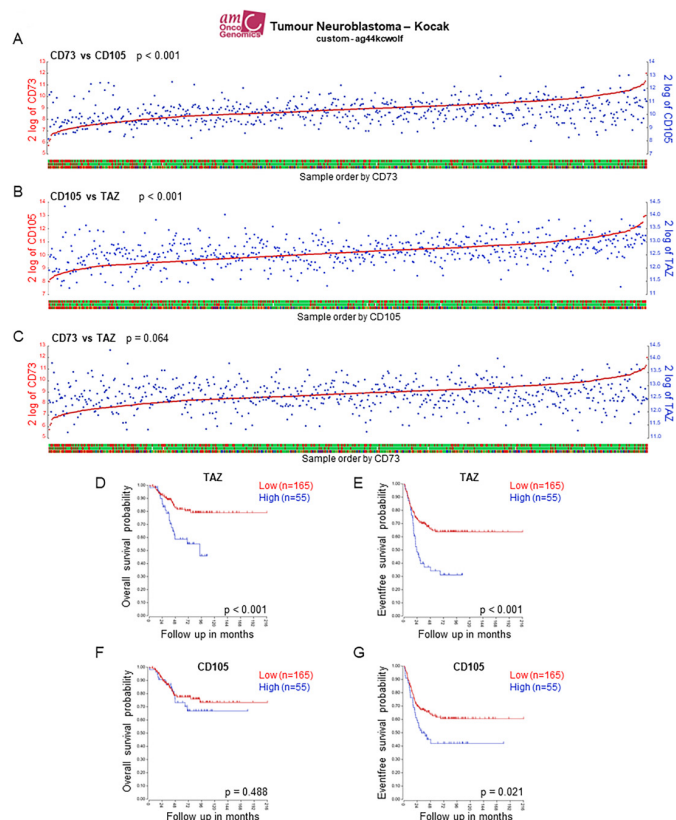
To confirm these results, we performed a gene-expression analysis querying the R2 platform, a public gene-expression dataset, to assess the expression of CD105, CD73 and TAZ.

We found a significant correlation between the expression of CD105 and CD73 or TAZ (p<0.001) while there was only a trend between the expression of CD73 and TAZ (p=0.064) (figure 3A–C). We then used the same dataset to evaluate the impact of the expression of these markers on patient's OS and EFS. In the stage IV, non-MYCN-amplified group, a higher expression of TAZ (OS and EFS: p<0.001) and CD105 (EFS: p=0.021) was associated with poorer outcome (figure 3D–G). In addition, in the stage IV MYCN-amplified group, a higher expression of CD73 was associated with a poorer clinical outcome (OS: p<0.001; EFS: p=0.025) (online supplemental figure 1).

NB-MSC cell lines are resistant to NK cell-mediated lysis
Having confirmed the presence of NB-MSC subset also in tumor samples, we investigated whether these cells had any effect on antitumor responses mediated by NK cells.

We first analyzed the cytolytic activity of aNK cells against all five NB cell lines in 4 hours coculture assays. As shown in figure 4A, NB-MSC cell lines were resistant

Figure 3 Negative impact of the high expression of CD73, CD105 and TAZ on stage IV NB Using the public dataset R2 (Kocak, custom ag44kcwolf, n=649 cases) several analyses were performed. A correlation analysis between CD73 versus CD105 (A), CD105 versus TAZ (B) and CD73 versus TAZ (C) has been carried out. OS and EFS probabilities according to the level of expression (high versus low) of TAZ (D-E) and CD105 (F-G) in stage IV MYCN non-amplified NB has been performed using as cut-off the last quartile of the distribution. EFS, event-free survival; NB, neuroblastoma; OS, overall survival.

Figure 4 Susceptibility of NB-cell lines to NK-cell-mediated lysis. (A), Allogeneic aNK cells were used as effector cells against CMFDA-labeled NB cell lines used as targets at different E:T ratios. Data were expressed as mean±SD (n=6) of percent of cell lysis (PI+ cells). (B) Flow-cytometry analysis of surface B7-H6, PVR, Nectin-2, ULBP-2/5/6, ULBP-3, MIC-A/B and HLA class I molecules (HLA-A-B-C) in different NB cell lines. MFI ratio was expressed as mean±SD (n=4). (C) aNK cell-mediated cytotoxicity assays against SK-N-AS, SK-N-BE(2)C and HTLA-230 either in the presence or absence of anti B7-H3 masking mAb. Allogeneic aNK cells were used as effector cells against ^{51}Cr-labeled NB target cells at 10:1 and 5:1 E:T ratios. Anti-B7-H3 IgM (M5B14) or control IgM mAbs (Ctrl) were added to cultures. Data are expressed as fold changes in the percent lysis as compared with controls±SD (n=4). (D) aNK cell-mediated ADCC assays against the NB^{CD105+} cell lines SK-N-AS, SK-N-BE(2)C, SH-SY5Y or BM-MSC using an anti-CD105 IgG mAb, that induced ADCC, or irrelevant IgG mAb as control. Target cells were labeled with ^{51}Cr and allogeneic aNK cells used as effectors at different E:T ratios as indicated. BM-MSC were used as positive control. Data are expressed as fold changes of the percent lysis as compared with control ±SD (n=3). *P<0.05 vs Ctrl. ADCC, antibody-dependent cellular cytotoxicity; aNK, activated natural killer; BM-MSC, bone marrow-derived mesenchymal stromal cell; NB, neuroblastoma.
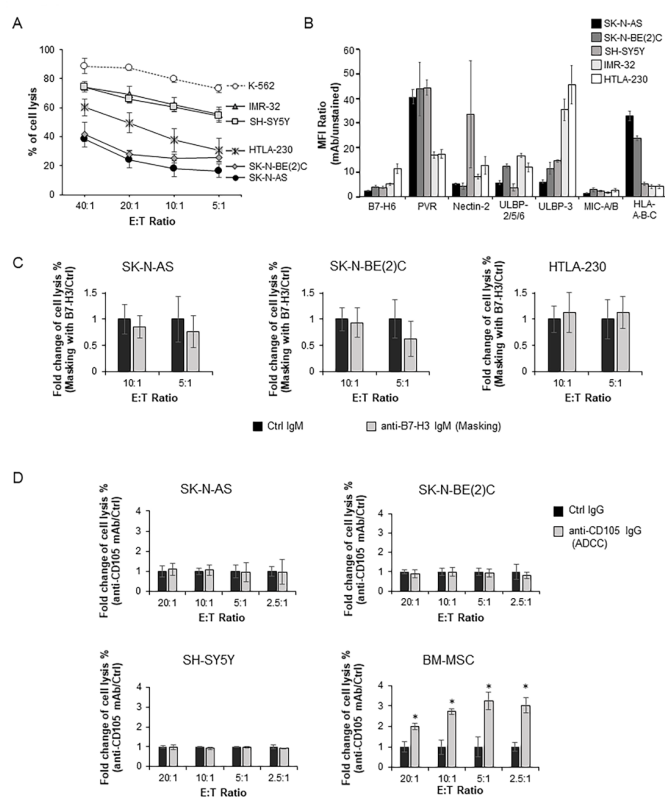
to lysis, while IMR-32 and SH-SY5Y cells were efficiently killed. HTLA-230 displayed an intermediate susceptibility.

We then analyzed NB cells for the expression of surface ligands for activating NK receptors, with particular focus on the expression of ligands of NKp30 (B7-H6), DNAM-1 (PVR and Nectin-2) and NKG2D (ULBP-2/5/6, ULBP-3 and MIC-A/B). In addition, we assessed the expression of HLA class I molecules recognized by the major HLA-class I-specific inhibitory receptors KIR and NKG2A (as shown in figure 4B). All NB cell lines expressed variable amounts of ligands of NK activating receptors.

Of note, the two NB-MSC cell lines, SK-N-AS and SK-N-BE (2)C, expressed high levels of HLA class I molecules (figure 4B), this representing an unusual feature in NB cells.[8 9] However, in agreement with data previously reported on different NB cell lines,[30] mAb-mediated masking of HLA class I molecules did not rescue the cytolytic activity of aNK cells against the two NB-MSC cell lines (data not shown).

We also attempted to improve the antitumor activity of aNK cells against NB-MSC cell lines by masking B7-H3, a surface molecule reported to interfere with the NK-cell-mediated lysis of NB cells, which is now under investigation in a clinical trial for the treatment of patients with refractory NB.[26 31–33] However, the NK-cell-mediated lysis of SK-N-AS, SK-N-BE-(2)C and HTLA-230 cells was not increased on mAb-mediated masking of B7-H3 (figure 4C).
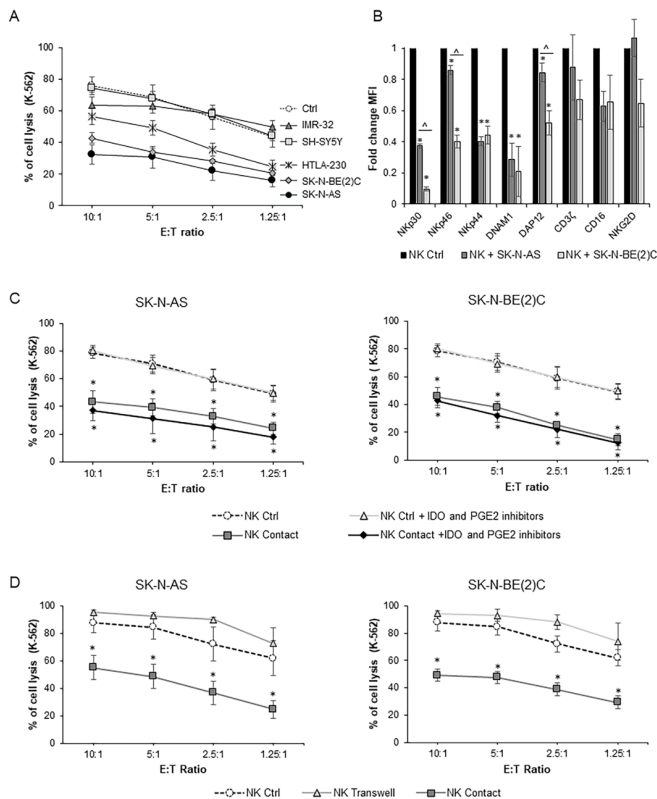
Figure 5 Evaluation of NK cell cytotoxic activity after coculture with NB cell lines. (A) NK cytotoxicity assays against CMFDA-labeled K-562 target cells were performed after 4 days coculture of freshly isolated PB NK cells either in the presence of different NB cell lines or alone (NK Ctrl). Percentages of cell lysis were expressed as mean±SD (n=6). (B) Flow-cytometry analysis of the activating or inhibitory receptors on NK cells after 4 days coculture with the indicated NB cells. Controls are NK cells cultured alone (NK Ctrl). Fold change MFI were expressed as mean±SD (n=3). *P<0.05 vs NK only. ∧P<0.05 between NK+SK-N-AS and NK+SK-N-BE(2)C. (C), Percentage of K-562 cells lysis in cytotoxicity assays using freshly isolated NK cells after 4 days coculture with SK-N-AS or SK-N-BE(2)C cell lines either in the presence or in the absence of IDO and PGE2 inhibitors (NK Contact and NK Contact+IDO and PGE2 inhibitors). NK cultured alone with or without inhibitors (NK Ctrl and NK Ctrl+IDO and PGE2 inhibitors) were used as controls. Values are expressed as mean±SD (n=3). *P<0.05 vs NK Ctrl and vs NK Ctrl+IDO and PGE2 inhibitors. (D) NK-cell cytotoxicity assays against CMFDA-labeled K-562 cells after 4 days coculture with SK-N-AS or SK-N-BE(2)C cell lines under transwell or cell-to-cell contact conditions. In this culture setting, freshly isolated NK cells were cultured in contact with SK-N-AS or SK-N-BE(2)C in the lower chamber (NK Contact) or in the upper chamber (NK Transwell). NK cultured alone for 4 days were used as control (NK Ctrl). Percentages of K-562 cells lysis are expressed as mean±SD (n=3). *P<0.05 vs NK Ctrl. IDO, indoleamine 2,3-dioxygenase; NB, neuroblastoma; NK, natural killer.

Similarly, coating the three CD105$^+$ NB cell lines SK-N-AS, SK-N-BE(2)C and SH-SY5Y with the anti-CD105 mAb (TRC105), which has been shown to mediate ADCC, did not induce target cell lysis (figure 4D). In control

experiments, TRC105 increased aNK cytolytic effects against non-neoplastic BM-derived MSCs, known to be susceptible to ADCC[34] (figure 4D). In addition, coating the above mentioned three NB cell lines with the anti-GD2 mAb dinutuximab beta which causes ADCC in vivo,[28 34] induced target cell lysis in SK-N-BE(2)C, but not in SK-N-AS and in SH-SY5Y used as control (online supplemental figure 2).

Overall, these data would indicate that NB-MSC display different mechanisms of resistance to NK-cell-mediated killing.

NB-MSC cell lines inhibit the cytolytic activity of NK cells

Next, we analyzed whether, on prolonged contact, NB cell lines could also interfere with the cytolytic activity of freshly isolated NK cells. Thus, at day 4 of coculture, NK cells were collected and tested for their cytolytic activity against K-562 (figure 5A). Both SK-N-AS and SK-N-BE(2)C cell lines strongly inhibited the cytolytic activity of cocultured NK cells, while HTLA-230 displayed only a mild inhibitory activity and IMR-32 and SH-SY5Y did not show any inhibitory effect.

We then analyzed whether the inhibitory effect was consequent to downregulation of activating NK receptors (figure 5B). In agreement with previous data on the effect of melanoma cell lines on NK cells, also NB-MSC cell lines induced a sharp decrease of the expression of natural cytotoxicity receptors (NCRs) on NK cells when cocultured with SK-N-AS and SK-N-BE(2)C as compared with controls. The decrease of NKp30 was 62.6%±1.2% and 90.4%±1.4% (p<0.001), that of NKp46 was 14.0%±2.9% (p<0.05) and 59.8%±4.1% (p<0.001), and that of NKp44 of 59.7%±2.9% and 55.6%±5.8% (p<0.001) in NK cocultured with SK-N-AS and SK-N-BE(2)C, respectively. In addition, also the expression of the adhesion and activating molecule DNAM1 and of the adaptor protein DAP12 were significantly decreased: DNAM1 by 71.4%±10.6% and 79.1%±16.3% (p<0.001) and DAP12 by 15.6%±5.0% and 47.9%±6.6%, respectively, in NK cocultured with SK-N-AS (p<0.05) and SK-N-BE(2)C in comparison to control NK cells grown in the absence of tumor cells (p<0.001). Although not significant, we observed a trend of decreased expression both for CD3ζ signaling polypeptide and for the activating receptor NKG2D when NK cells were cultured in the presence of SK-N-BE(2)C. CD16 showed a not statistically significant negative trend of expression on the NK cells cultured with both NB-MSC lines.

We further investigated whether the inhibitory effect on NK cells was mediated by soluble factors, possibly released during the interaction between NK and NB-MSC cells. To this purpose, we cocultured NB-MSC cells with freshly isolated NK cells for 4 days in the presence of specific inhibitors of IDO and PGE2, two important immunosuppressive mediators often present in the TME. At the end of cocultures, NK cells were tested for their ability to lyse K-562. No significant difference in the NK cell lytic activity was detected in the presence of IDO and PGE2

inhibitors, suggesting that these two molecules are not involved in suppression of NK cell mediated by NB-MSCs (figure 5C). For further investigating the possible involvement of soluble inhibitory factors, we used in vitro transwell coculture conditions in which the upper chamber contained freshly isolated NK cells (NK Transwell) that were separated by a porous membrane allowing the passage of diffusible factors, from NB cells cocultured with freshly isolated NK cells (NK Contact). Freshly isolated NK cells cultured alone were used as control (NK Ctrl). After 4 days of culture, no significant decrease of cytolytic activity was detected in NK cells harvested from the upper chamber (NK Transwell) as compared with NK Ctrl, whereas the NK cells kept in contact with NB-MSC were strongly inhibited (figure 5D).

Similar results were obtained in transwell cocultures with NK cells in the upper chamber and NB-MSC cells in the lower chamber without NK cell contact (data not show).

These data suggest that the inhibition of the NK cell cytotoxicity is not the result of soluble inhibitory molecules released and diffused from NB cells, but rather requires NB-MSC-NK cell contact.

TAZ silencing reduces the capability of SK-N-AS to inhibit NK-cell cytotoxicity

In an attempt to clarify the molecular mechanism(s) responsible for NB-MSC resistance to NK-mediated killing, we investigated whether silencing of the immune-regulatory molecules CD73 and TAZ in NB-MSC cells could result in the recovery of their susceptibility to NK cell-mediated lysis. We could successfully downregulate these two molecules in SK-N-AS by siRNA transfection (transfection resulted poorly efficient in SK-N-BE(2)C cells). Functional studies were performed 3 days after transfection at the time when maximal protein inhibition was detected (figure 6A,B; online supplemental figure 3A). Notably, silencing of CD73 or TAZ did not affect the cytolytic potential of aNK cells against SK-N-AS (online supplemental figure 3B) and figure 6C). We then evaluated the impact of siRNA silencing on the immunomodulatory capability of NB-MSCs. Thus, SK-N-AS were transfected with siRNA-CD73, siRNA-TAZ or siRNA-Ctrl and, starting at day 3 post-transfection, they were cocultured for 4 days with freshly isolated NK cells. NK cells were then collected and analyzed in a cytotoxicity assay against K-562. Cocultures with siRNA-CD73+ SK-N-AS did not modify cytotoxic potential of NK cells (online supplemental figure 3C), while cocultures with siRNA-TAZ+ SK-N-AS resulted in a significant increase (p<0.05) of lytic activity as compared with siRNA-Ctrl cells at all E:T ratios. Similar results were obtained using two different siRNA oligonucleotides directed against TAZ, confirming the reliability of the data (figure 6D). As further effect of the siRNA-TAZ, we found an upregulation of NCRs in NK cells, a result in line with the increase of NK-mediated lysis of SK-N-AS NB cells (data not shown).

Subsequently, we analyzed the expression of different molecular targets[20] of TAZ on SK-N-AS by RT-qPCR before and after coculture at day 3 and 7 post-transfection, including the platelet derived growth factor-β (PDGFβ), the programmed death-ligand 1 and 2 (PD-L1 and PD-L2) and the sphingosine 1-phosphate receptor 1 (S1RP1).

Data shown in figure 6E revealed that TAZ mRNA was significantly lower in siRNA-TAZ SK-N-AS as compared with siRNA-Ctrl (p<0.001) during the entire coculture period. Furthermore, the amount of PDGFβ transcript was significantly reduced with an average decrease of 35.9%±0.6% at day 3 and 19.8%±6.6% at day 7 (p<0.001). The reduction of PD-L1 was also statistically significant in siRNA-TAZ as compared with siRNA-Ctrl: 25.0%±1.2% at day 3 and 46.8%±8.6% at day 7 (p<0.001). Similarly, the average reduction of PD-L2 expression was 34.9%±7.1% and 33.9%±12.1% at day 3 and 7, respectively. S1RP1 reduction was 11.7%±4.2% and 33.0%±6.4% at day 3 and 7, respectively (p<0.05).

These results indicate that the inhibitory effect of TAZ acts on downstream target genes and its silencing upregulates NCRs, thus further reducing the overall inhibitory capacity of SK-N-AS on NK cells.

TAZ overexpression increases the capability of SH-SY5Y to inhibit NK-cell cytotoxicity

Transient transfection of SH-SY5Y with a TAZ expression vector caused a strong overexpression of the TAZ mRNA and protein up to 72 hours (figure 7A). Notably, RT-PCR analysis (figure 7B) shows striking upregulation of PDGFβ, PD-L1 and S1RP1 transcripts correlated with TAZ overexpression, indicating that the transfected TAZ protein is functional. In these experimental conditions, functional studies revealed that in SH-SY5Y cells overexpression of TAZ did not affect their susceptibility to direct NK lysis (figure 7C), while NK cells cocultured with SH-SY5Y overexpressing TAZ (figure 7D), exhibited a small but statistically significant (p<0.05) decreased cytotoxic activity against K562 target cells. Overall, these data strengthen the role of TAZ in the control of NK cells functions.

DISCUSSION

In the present study, we show that cells with mesenchymal characteristics present in NB TME may be of both neoplastic and stromal origin,[12 13] both displaying immunosuppressive properties that may favor the emergence of tumor immune-escape pathways. Although several immunosuppressive mechanisms have been reported in NB,[8 9] to the best of our knowledge, no tumor MSC-like cells displaying such properties have been identified so far. In this context, van Groningen et al[15] reported that NB is composed of two tumor cell subsets with divergent gene expression profiles, namely committed adrenergic cells and primitive uncommitted cells identified according to the expression of CD133. The latter are chemoresistant in vitro and appear to be enriched in tumor relapse
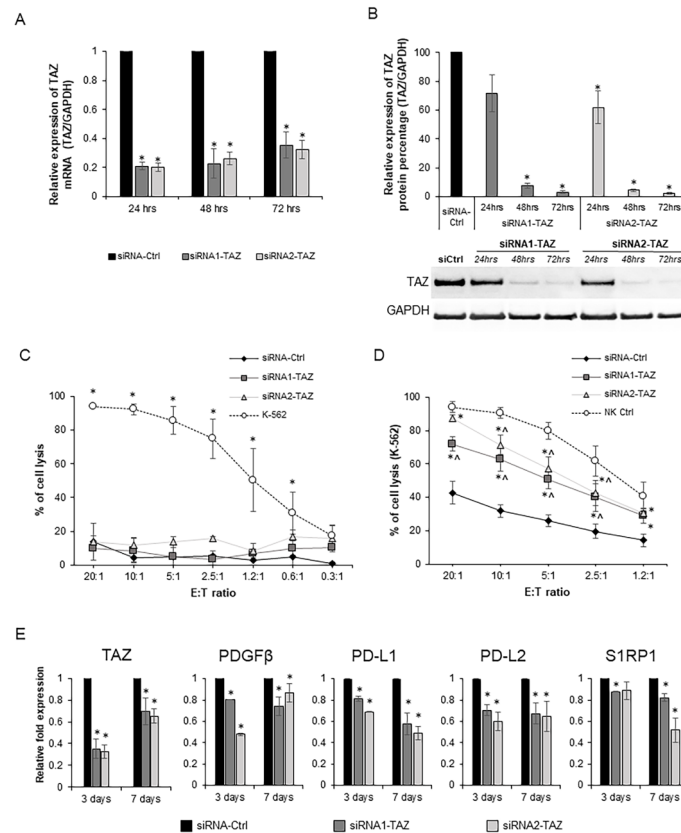
Figure 6 Effect of TAZ silencing on SK-N-AS cell line mediated inhibition of NK cell cytotoxicity. (A) Relative expression of TAZ mRNA normalized on GAPDH expression in SK-N-AS after transfection with siRNA1-TAZ, siRNA2-TAZ and siRNA-Ctrl, at different time point, by RT-qPCR. Data are expressed as mean±SD (n=3). *P<0.05 vs siRNA-Ctrl. (B) WB of TAZ expression in SK-N-AS after transfection with siRNA1-TAZ, siRNA2-TAZ and siRNA-Ctrl, at different time points. GAPDH was used as loading control. Histograms represent densitometry analysis of TAZ protein normalized on GAPDH protein expression. Data are expressed as mean±SD (n=3) (upper panel). A representative WB experiment is shown (lower panel). *P<0.05 vs siRNA-Ctrl. (C) aNK cell cytotoxicity assays against transfected SK-N-AS or K-562 cells labeled with CMFDA. SK-N-AS were transfected with siRNA1-TAZ, siRNA2-TAZ or siRNA-Ctrl and after 3 days were used as target in a cytotoxicity assay. K-562 cells were used as control target. Percentages of cell lysis are expressed as mean±SD (n=3). *P<0.05 K-562 vs siRNA SK-NAS cells. (D) NK cell cytotoxicity assays on 4 days coculture with SK-N-AS transfected with siRNA1-TAZ, siRNA2-TAZ and siRNA-Ctrl. NK cultured alone used as controls (NK Ctrl). Three days after transfection, SK-N-AS were cultured with freshly isolated NK cells for 4 days. Then, NK cells were analyzed for their cytotoxic capacity against K-562 target cells. Percentage lysis of CMFDA labeled-K-562 cells was expressed as mean±SD (n=3). *P<0.05 vs siRNA-Ctrl; ∧p<0.05 vs NK Ctrl. (E) Expression of the indicated genes in SK-N-AS after transfection with siRNA1-TAZ, siRNA2-TAZ and siRNA-Ctrl, at different time point, is evaluated by RT-qPCR. GAPDH expression is used as reference gene. Data are expressed as fold changes compared with siRNA-Ctrl. Values indicate mean±SD (n=3). *P<0.05 vs siRNA-Ctrl. NK, natural killer.

samples.[15] However, the immune-regulatory activity of this subset has not yet been explored.

We hypothesized that NB could contain tumor cells with an immune-regulatory MSC phenotype. To prove this hypothesis, we used NK lymphocytes as effectors cells exploiting their ability to kill tumor cells. Five NB cell lines were analyzed for the expression of a large panel of MSC markers in order to identify cells with a MSC phenotype. Two out of five NB cell lines (SK-N-AS and SK-N-BE (2) C) were found to display: (i) phenotype and function typical of healthy BM-MSC, (ii) high resistance to NK-mediated killing and (iii) capacity to efficiently inhibit the cytotoxicity of aNK cells by cell-to-cell contact. In addition, we found that such inhibition occurred at least in part through a TAZ-dependent mechanism.

Different from previous data using adrenergic NB-cell lines,[30 35] the two identified NB-MSC cell lines were resistant to NK-mediated killing. Of particular relevance, CD105 mAb did not mediate ADCC using aNK cells as effector and NB-MSC as target cells. On the other hand, anti-GD2 mab mediated ADCC against SK-N-BE (2) C cells but not against SK-N-AS cells highlighting a heterogeneous response within NB-MSC cells. In this context, recent data reported that ADCC against CD105^{+} or GD2^{+} cells is important for tumor eradication in vivo and provides a promising immunotherapeutic tool.[34] However, this therapeutic approach may be ineffective in case of resistant NB-MSC-like cells.[34]

It is important to underline that the immune-regulatory effects of NB-MSC are likely to affect other effectors
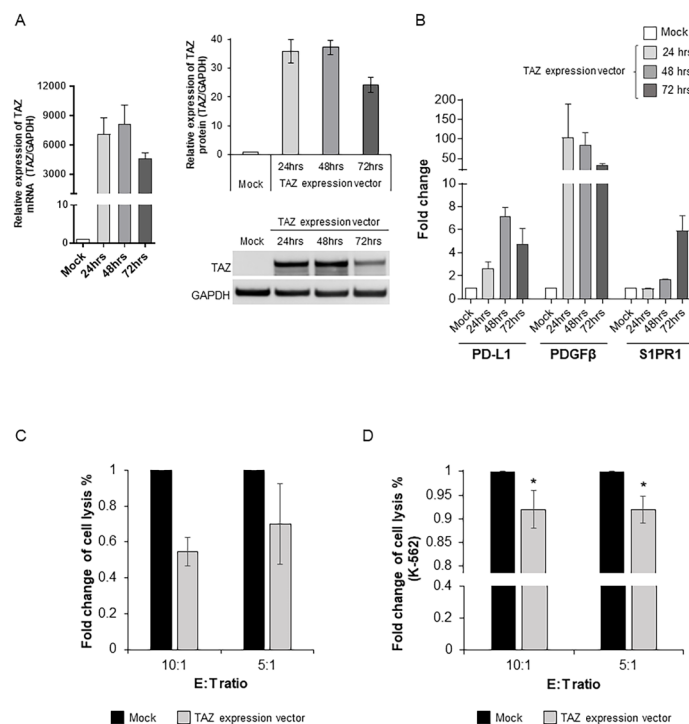
Figure 7 Effect of TAZ overexpression on immunomodulatory properties of SH-SY5Ycells. (A,) Analysis of TAZ mRNA by RT-qPCR (*left panel*) and protein expression by WB (*right panel*) at different time points (24 hours, 48 hours, 72 hours) on transfected SH-SY5Y cells. Cells transfected without TAZ expression vector were used as mock control. Similar results were obtained using transfected cells with a vector encoding GFP only as mock control (data not shown). GAPDH was used as reference gene in RT-qPCR and as loading control in WB analysis. RT- qPCR data are expressed as fold change as compared with control at the same time point. Histograms above WB represent densitometry for the relative quantification of TAZ protein expression normalized for GAPDH. Data are expressed as mean±SD (n=3). A representative WB experiment is shown. (B,) Expression of the indicated genes in SH-SY5Y after transfection with TAZ expression vector compared with Mock control at different time point, is evaluated by RT-qPCR. GAPDH expression is used as reference gene. Data are expressed as fold changes compared with Mock control. Values indicate mean±SD (n=3). (C) aNK cell-mediated cytotoxicity assays against SH-SY5Y labeled with CMFDA. SH-SY5Y were transfected with TAZ expression vector or plasmid vector encoding GFP only (Mock) and after 48 hours was used as target in a cytotoxicity assay at 10:1 and 5:1 E:T ratios. Data are expressed as fold changes of cell lysis percent compared with controls (Mock) ±SE (n=3). (D), NK-cell cytotoxicity assays against CMFDA-labeled K-562 cells on coculture with SH-SY5Y transfected with TAZ expression vector or plasmid vector encoding GFP only (Mock). 24-hour days after transfection, SH-SY5Y were cultured in contact with freshly isolated NK cells for 4 days. Then, NK cells were analyzed for their cytotoxic capacity against K-562 used as control target cells at 10:1 and 5:1 E:T ratios. Percentage lysis of CMFDA labelled-K-562 cells were expressed as fold changes of cell lysis percent compared with controls (Mock)±SE (n=3). *$P<0.05$ vs Mock. aNK, activated natural killer.

besides NK cells, including T lymphocytes. Accordingly, also sophisticated cell-based immunotherapies, including chimeric antigen receptor-engineered T cells could be inhibited by this pathway.[36–38]

Regarding the molecular mechanisms underlying the immune-suppressive activity of NB-MSC these may involve p53, as both cell lines display p53 mutations,[39] a parameter that has recently been associated with a poor susceptibility to NK-cell-mediated killing of NB cell lines.[40]

Decreased expression or functional impairment of activating receptors, coreceptors and adaptor signaling molecules are frequent tumor-induced mechanisms leading to inhibition of NK-cell-mediated cytotoxicity against a wide variety of tumor cells.[41 42] Coculture with NB-MSCs could induce a significantly decreased expression of activating receptors on NK cells, particularly NCRs, DNAM1 and

the DAP12 adaptor signaling polypeptide. This finding strongly suggests that downregulation of these receptors plays an important role in the impaired cytotoxic potential of NK cells. A number of studies suggested the existence of different NCR ligands on tumor cells. Accordingly, the inhibition of different NCR by using a combination of specific neutralizing mAbs resulted in a more efficient blocking of NK-cell-mediated tumor cell lysis as compared with the mAbs used individually.[43] The decreased expression of NCRs and DNAM1 may be caused by the persistent contact with their ligands. In this context, while downregulation of NCR can be induced by both membrane and soluble ligands, in the case of DNAM1, it is strictly dependent on cell–cell contact.[43] This mechanism is likely involved in the inhibitory activity exerted by NB-MSC on the cytotoxic activity of NK cells.

In order to identify molecular mechanism(s) underlying the NB-MSC-mediated cytotoxic dysfunction of NK cells, we focused on CD73 and TAZ. Extracellular adenosine generated by the ectonucleotidase CD73 is a newly recognized "immune checkpoint mediator" that interferes with antitumor immune responses. In addition, studies performed in several human malignancies demonstrated that high levels of CD73 expression in the TME are associated with a worse clinical outcome.[44] We obtained similar evidence in NBs, since in the stage IV MYCN-amplified group, a higher expression of CD73 was associated with a poorer clinical outcome. On the other hand, TAZ is a fundamental member of the Hippo signaling pathway[17–19 45] that could affect tumor immunity by regulating the interactions between immune and tumor cells taking place primarily in the TME.[17] In NB, TAZ activation has been reported to positively correlate with adverse prognostic features.[46]

The influence of CD73 and TAZ on the cross-talk between NB and NK cells was poorly defined;[18] therefore, we investigated whether CD73 and TAZ silencing could modify NB-MSC/NK cell interactions. In our setting, CD73 silencing did not affect NK functions; however, it is conceivable that CD73 expressed by NB-MSC cells could display regulatory properties on other immune cells present in the NB TME. By contrast, concerning TAZ, its silencing did not modify NB-MSC susceptibility to a NK-mediated killing, whereas the cytotoxic potential of freshly isolated NK cells was restored possibly reflecting the upregulation of NCRs that plays an important role in NK-mediated tumor cell killing.[43] In addition, TAZ silencing in NB-MSC cells induced downregulation of different molecules with immune-suppressive activity on NK-cell function, including PDGFβ, PD-L1 and PD-L2.[47 48] Conversely, SH-SY5Y cells overexpressing TAZ exhibited a concomitant overexpression of PD-L1, PDGFβ and S1PR1 transcripts and NK cells cocultured with these transfected SH-SY5Y cells displayed a small but statistically significant decreased capacity to kill K562 target cells. Overall, these data highlight the unprecedented capacity of TAZ to control NK cells cytotoxic functions.

While PD1$^+$ NK cells are present in low proportions in the peripheral blood, their proportions in TME may be substantially higher;[48 49] thus, TAZ-silencing-induced decreased expression of PD-L1 and PD-L2 on tumor cells could be involved in the increased efficiency of NK-cell cytotoxicity at the tumor site.[50–52] In addition, PDGFβ that may be present in a membrane-bound form in cancer cells[53] efficiently inhibits the cytotoxic function of NK cells.[47] Being controlled by TAZ[21] PDGFβ may represent a candidate for the requirement of contact between NB-MSC and NK cells to obtain inhibition.

It has been shown that overexpression of TAZ increases NB-cell proliferation and colony formation,[17 18] while YAP/TAZ-mediated expression of PD-L1 could result in inhibition of T-cell function.[17 18] Therefore, such TAZ-dependent effects, together with our present demonstration of TAZ-mediated inhibition of NK cytotoxic activity,

may help explain why TAZ activation in vivo is positively correlated with poor clinical outcome,[46] thus providing a useful prognostic tool in stage IV NB.

While our present study is based on the analysis of a limited number of cell lines, we could perform IHC analysis on 33 primary NB samples. In addition, our data are supported by data from a public gene-expression dataset. In conclusion, our study allows better understanding NB pathophysiology and helping design preclinical and clinical studies aimed at improving the clinical outcome of patients with highly aggressive NB.

CONCLUSION

We identified a novel immune-regulatory subset of NB cells that displays phenotypic and functional properties of MSC. These cells display multifactorial resistance to NK-cell-induced killing and efficiently inhibit, on coculture, NK-cell cytotoxic activity against tumor cells. This property appears to be regulated by the transcriptional coactivator TAZ whose effect on NK-cell function has been neglected so far.[17 18] Our data offer novel cellular and molecular targets whose inhibition could lead to more efficient immunotherapy of NB.

Author affiliations
[1]Immunology Area, Bambino Gesù Children's Hospital, IRCCS, Rome, Italy
[2]Pathology Department, IRCCS Sacro Cuore Don Calabria, Negrar, Verona, Veneto, Italy
[3]Department of Molecular and Translational Medicine, University of Brescia, Brescia, Italy
[4]Core Facilities, Bambino Gesù Children's Hospital, IRCCS, Rome, Italy
[5]Tracon Pharmaceuticals, Inc, San Diego, California, USA
[6]Anatomical Pathology Area, Bambino Gesù Children's Hospital, IRCCS, Rome, Italy
[7]Department of Paediatric Haematology and Oncology, Cell and Gene Therapy, Bambino Gesù Children's Hospital, IRCCS, Rome, Italy
[8]Department of Gynaecology/Obstetrics and Paediatrics, Sapienza, University of Rome, Rome, Italy
[9]Department of Paediatric Haematology, Oncology and Stem Cell Transplantation University Children's Hospital of Würzburg, Würzburg, Germany

Ethics approval The use of human overflow paraffin-embedded NB tissues was approved by our local Institutional Review Board and the research protocol was approved by the Ethics Committees of the IRCCS Bambino Gesù Children's Hospital (OPBG, 1626/2018).

Provenance and peer review Not commissioned; externally peer reviewed.

Data availability statement All data relevant to the study are included in the article or uploaded as supplementary information.

Supplemental material This content has been supplied by the author(s). It has not been vetted by BMJ Publishing Group Limited (BMJ) and may not have been peer-reviewed. Any opinions or recommendations discussed are solely those of the author(s) and are not endorsed by BMJ. BMJ disclaims all liability and responsibility arising from any reliance placed on the content. Where the content includes any translated material, BMJ does not warrant the accuracy and reliability of the translations (including but not limited to local regulations, clinical guidelines, terminology, drug names and drug dosages), and is not responsible for any error and/or omissions arising from translation and adaptation or otherwise.

Open access This is an open access article distributed in accordance with the Creative Commons Attribution Non Commercial (CC BY-NC 4.0) license, which permits others to distribute, remix, adapt, build upon this work non-commercially, and license their derivative works on different terms, provided the original work is properly cited, appropriate credit is given, any changes made indicated, and the use is non-commercial. See http://creativecommons.org/licenses/by-nc/4.0/.

ORCID iDs
Andrea Pelosi http://orcid.org/0000-0003-2308-9215
Sabina Di Matteo http://orcid.org/0000-0002-2586-7159
Ignazio Caruana http://orcid.org/0000-0002-9250-0605
Bruno Azzarone http://orcid.org/0000-0002-5962-3849

REFERENCES

1. Maris JM. Recent advances in neuroblastoma. *N Engl J Med* 2010;362:2202–11.
2. Cheung N-KV, Dyer MA. Neuroblastoma: developmental biology, cancer genomics and immunotherapy. *Nat Rev Cancer* 2013;13:397–411.
3. Cohn SL, Pearson ADJ, London WB, *et al*. The International neuroblastoma risk group (INRG) classification system: an INRG Task force report. *J Clin Oncol* 2009;27:289–97.
4. Matthay KK, Maris JM, Schleiermacher G, *et al*. Neuroblastoma. *Nat Rev Dis Primers* 2016;2:16078.
5. Moreno L, Rubie H, Varo A, *et al*. Outcome of children with relapsed or refractory neuroblastoma: a meta-analysis of ITCC/SIOPEN European phase II clinical trials. *Pediatr Blood Cancer* 2017;64:25–31.
6. Yu AL, Gilman AL, Ozkaynak MF, *et al*. Anti-Gd2 antibody with GM-CSF, interleukin-2, and isotretinoin for neuroblastoma. *N Engl J Med* 2010;363:1324–34.
7. Caruana I, Weber G, Ballard BC, *et al*. K562-derived whole-cell vaccine enhances antitumor responses of CAR-redirected virus-specific cytotoxic T Lymphocytes in *Vivo*. *Clin Cancer Res* 2015;21:2952–62.
8. Bottino C, Dondero A, Bellora F, *et al*. Natural killer cells and neuroblastoma: tumor recognition, escape mechanisms, and possible novel immunotherapeutic approaches. *Front Immunol* 2014;5:56.
9. Pistoia V, Morandi F, Bianchi G, *et al*. Immunosuppressive microenvironment in neuroblastoma. *Front Oncol* 2013;3:167.
10. Gascard P, Tlsty TD. Carcinoma-associated fibroblasts: orchestrating the composition of malignancy. *Genes Dev* 2016;30:1002–19.
11. Galland S, Vuille J, Martin P, *et al*. Tumor-derived mesenchymal stem cells use distinct mechanisms to block the activity of natural killer cell subsets. *Cell Rep* 2017;20:2891–905.
12. Borriello L, Nakata R, Sheard MA, *et al*. Cancer-associated fibroblasts share characteristics and protumorigenic activity with mesenchymal stromal cells. *Cancer Res* 2017;77:5142–57.
13. Pelizzo G, Veschi V, Mantelli M, *et al*. Microenvironment in neuroblastoma: isolation and characterization of tumor-derived mesenchymal stromal cells. *BMC Cancer* 2018;18:1176.
14. Royer-Pokora B, Busch M, Beier M, *et al*. Wilms tumor cells with WT1 mutations have characteristic features of mesenchymal stem cells and express molecular markers of paraxial mesoderm. *Hum Mol Genet* 2010;19:1651–68.
15. van Groningen T, Koster J, Valentijn LJ, *et al*. Neuroblastoma is composed of two super-enhancer-associated differentiation states. *Nat Genet* 2017;49:1261–6.
16. Wang Q, Xu Z, An Q, *et al*. Taz promotes epithelial to mesenchymal transition via the upregulation of connective tissue growth factor expression in neuroblastoma cells. *Mol Med Rep* 2015;11:982–8.
17. Pan Z, Tian Y, Cao C, *et al*. The emerging role of YAP/TAZ in tumor immunity. *Mol Cancer Res* 2019;17:1777–86.
18. Nguyen CDK, Yi C. Yap/Taz signaling and resistance to cancer therapy. *Trends Cancer* 2019;5:283–96.
19. Moroishi T, Hayashi T, Pan W-W, *et al*. The Hippo pathway kinases LATS1/2 suppress cancer immunity. *Cell* 2016;167:1525–39.
20. Janse van Rensburg HJ, Azad T, Ling M, *et al*. The Hippo pathway component TAZ promotes immune evasion in human cancer through PD-L1. *Cancer Res* 2018;78:1457–70.
21. Wang M, Liu Y, Zou J, *et al*. Transcriptional co-activator TAZ sustains proliferation and tumorigenicity of neuroblastoma by targeting CTGF and PDGF-β. *Oncotarget* 2015;6:9517–30.
22. Cordenonsi M, Zanconato F, Azzolin L, *et al*. The Hippo transducer TAZ confers cancer stem cell-related traits on breast cancer cells. *Cell* 2011;147:759–72.
23. Spaggiari GM, Capobianco A, Becchetti S, *et al*. Mesenchymal stem cell-natural killer cell interactions: evidence that activated NK cells are capable of killing MscS, whereas MscS can inhibit IL-2-induced NK-cell proliferation. *Blood* 2006;107:1484–90.
24. Cifaldi L, Romania P, Falco M, *et al*. Erap1 regulates natural killer cell function by controlling the engagement of inhibitory receptors. *Cancer Res* 2015;75:824–34.
25. Spaggiari GM, Capobianco A, Abdelrazik H, *et al*. Mesenchymal stem cells inhibit natural killer-cell proliferation, cytotoxicity, and cytokine production: role of indoleamine 2,3-dioxygenase and prostaglandin E2. *Blood* 2008;111:1327–33.
26. Castriconi R, Dondero A, Augugliaro R, *et al*. Identification of 4Ig-B7-H3 as a neuroblastoma-associated molecule that exerts a protective role from an NK cell-mediated lysis. *Proc Natl Acad Sci U S A* 2004;101:12640–5.
27. Ciccone E, Pende D, Nanni L, *et al*. General role of HLA class I molecules in the protection of target cells from lysis by natural killer cells: evidence that the free heavy chains of class I molecules are not sufficient to mediate the protective effect. *Int Immunol* 1995;7:393–400.
28. Barry WE, Jackson JR, Asuelime GE, *et al*. Activated natural killer cells in combination with anti-GD2 antibody Dinutuximab improve survival of mice after surgical resection of primary neuroblastoma. *Clin Cancer Res* 2019;25:325–33.
29. Bao Y, Nakagawa K, Yang Z, *et al*. A cell-based assay to screen stimulators of the Hippo pathway reveals the inhibitory effect of dobutamine on the YAP-dependent gene transcription. *J Biochem* 2011;150:199–208.
30. Sivori S, Parolini S, Marcenaro E, *et al*. Involvement of natural cytotoxicity receptors in human natural killer cell-mediated lysis of neuroblastoma and glioblastoma cell lines. *J Neuroimmunol* 2000;107:220–5.
31. Castellanos JR, Purvis IJ, Labak CM, *et al*. B7-H3 role in the immune landscape of cancer. *Am J Clin Exp Immunol* 2017;6:66–75.
32. Kramer K, Kushner BH, Modak S, *et al*. Compartmental intrathecal radioimmunotherapy: results for treatment for metastatic CNS neuroblastoma. *J Neurooncol* 2010;97:409–18.
33. Xu H, Cheung IY, Guo H-F, *et al*. Microrna miR-29 modulates expression of immunoinhibitory molecule B7-H3: potential implications for immune based therapy of human solid tumors. *Cancer Res* 2009;69:6275–81.
34. Wu H-W, Sheard MA, Malvar J, *et al*. Anti-CD105 antibody eliminates tumor microenvironment cells and enhances anti-GD2 antibody immunotherapy of neuroblastoma with activated natural killer cells. *Clin Cancer Res* 2019;25:4761–74.
35. Castriconi R, Dondero A, Cilli M, *et al*. Human NK cell infusions prolong survival of metastatic human neuroblastoma-bearing NOD/SCID mice. *Cancer Immunol Immunother* 2007;56:1733–42.
36. Caruana I, Diaconu I, Dotti G. From monoclonal antibodies to chimeric antigen receptors for the treatment of human malignancies. *Semin Oncol* 2014;41:661–6.
37. Ramakrishna S, Barsan V, Mackall C. Prospects and challenges for use of CAR T cell therapies in solid tumors. *Expert Opin Biol Ther* 2020;20:503–16.
38. Wang E, Wang L-C, Tsai C-Y, *et al*. Generation of potent T-cell immunotherapy for cancer using DAP12-Based, multichain, chimeric immunoreceptors. *Cancer Immunol Res* 2015;3:815–26.
39. Nakamura Y, Ozaki T, Niizuma H, *et al*. Functional characterization of a new p53 mutant generated by homozygous deletion in

a neuroblastoma cell line. *Biochem Biophys Res Commun* 2007;354:892–8.

40 Ray AK, Somanchi SS, Dastgheyb N, *et al*. Expression of carcinoma, apoptosis, and cell-death-related genes are determinants for sensitivity of pediatric cancer cell lines to lysis by natural killer cells. *Pediatr Blood Cancer* 2019;66:e27783.

41 Coudert JD, Zimmer J, Tomasello E, *et al*. Altered NKG2D function in NK cells induced by chronic exposure to NKG2D ligand-expressing tumor cells. *Blood* 2005;106:1711–7.

42 Thompson TW, Kim AB, Li PJ, *et al*. Endothelial cells express NKG2D ligands and desensitize antitumor NK responses. *Elife* 2017;6. doi:10.7554/eLife.30881. [Epub ahead of print: 12 Dec 2017].

43 Molfetta R, Quatrini L, Santoni A, *et al*. Regulation of NKG2D-dependent NK cell functions: the yin and the Yang of receptor endocytosis. *Int J Mol Sci* 2017;18. doi:10.3390/ijms18081677. [Epub ahead of print: 02 Aug 2017].

44 Allard B, Longhi MS, Robson SC, *et al*. The ectonucleotidases CD39 and CD73: novel checkpoint inhibitor targets. *Immunol Rev* 2017;276:121–44.

45 Zhou X, Lei Q-Y. Regulation of TAZ in cancer. *Protein Cell* 2016;7:548–61.

46 Ahmed AA, Mohamed AD, Gener M, *et al*. Yap and the Hippo pathway in pediatric cancer. *Mol Cell Oncol* 2017;4:e1295127.

47 Gersuk GM, Westermark B, Mohabeer AJ, *et al*. Inhibition of human natural killer cell activity by platelet-derived growth factor (PDGF). III. membrane binding studies and differential biological effect of recombinant PDGF isoforms. *Scand J Immunol* 1991;33:521–32.

48 Pesce S, Greppi M, Grossi F, *et al*. PD/1-PD-Ls checkpoint: insight on the potential role of NK cells. *Front Immunol* 2019;10:1242.

49 Beldi-Ferchiou A, Lambert M, Dogniaux S, *et al*. Pd-1 mediates functional exhaustion of activated NK cells in patients with Kaposi sarcoma. *Oncotarget* 2016;7:72961–77.

50 Obeid JM, Erdag G, Smolkin ME, *et al*. Pd-L1, PD-L2 and PD-1 expression in metastatic melanoma: correlation with tumor-infiltrating immune cells and clinical outcome. *Oncoimmunology* 2016;5:e1235107.

51 Dondero A, Pastorino F, Della Chiesa M, *et al*. Pd-L1 expression in metastatic neuroblastoma as an additional mechanism for limiting immune surveillance. *Oncoimmunology* 2016;5:e1064578.

52 Yang H, Zhou X, Sun L, *et al*. Correlation between PD-L2 expression and clinical outcome in solid cancer patients: a meta-analysis. *Front Oncol* 2019;9:47.

53 Ho IAW, Toh HC, Ng WH, *et al*. Human bone marrow-derived mesenchymal stem cells suppress human glioma growth through inhibition of angiogenesis. *Stem Cells* 2013;31:146–55.